MOLECULAR AND CELLULAR BIOLOGY, Oct. 2010, p. 4851–4863 Vol. 30, No. 20
0270-7306/10/$12.00 doi:10.1128/MCB.00521-10

Lysine-Specific Demethylase 1 Regulates the Embryonic Transcriptome and CoREST Stability▽†

Charles T. Foster,[1] Oliver M. Dovey,[1] Larissa Lezina,[1] Jin Li Luo,[2] Timothy W. Gant,[2] Nick Barlev,[1] Allan Bradley,[3] and Shaun M. Cowley[1]*

Department of Biochemistry, Henry Wellcome Building, Lancaster Road, University of Leicester, Leicester LE1 9HN, United Kingdom[1]; Systems Toxicology Group, MRC Toxicology Unit, Hodgkin Building, Lancaster Road, Leicester LE1 9HN, United Kingdom[2]; and Wellcome Trust Sanger Institute, Hinxton, Cambridge CB10 1SA, United Kingdom[3]

Received 5 May 2010/Returned for modification 12 June 2010/Accepted 7 August 2010

Lysine-specific demethylase 1 (LSD1), which demethylates mono- and dimethylated histone H3-Lys4 as part of a complex including CoREST and histone deacetylases (HDACs), is essential for embryonic development in the mouse beyond embryonic day 6.5 (e6.5). To determine the role of LSD1 during this early period of embryogenesis, we have generated loss-of-function gene trap mice and conditional knockout embryonic stem (ES) cells. Analysis of postimplantation gene trap embryos revealed that LSD1 expression, and therefore function, is restricted to the epiblast. Conditional deletion of LSD1 in mouse ES cells, the *in vitro* counterpart of the epiblast, revealed a reduction in CoREST protein and associated HDAC activity, resulting in a global increase in histone H3-Lys56 acetylation, but not H3-Lys4 methylation. Despite this biochemical perturbation, ES cells with LSD1 deleted proliferate normally and retain stem cell characteristics. Loss of LSD1 causes the aberrant expression of 588 genes, including those coding for transcription factors with roles in anterior/posterior patterning and limb development, such as brachyury, Hoxb7, Hoxd8, and retinoic acid receptor γ (RARγ). The gene coding for brachyury, a key regulator of mesodermal differentiation, is a direct target gene of LSD1 and is overexpressed in e6.5 *Lsd1* gene trap embryos. Thus, LSD1 regulates the expression and appropriate timing of key developmental regulators, as part of the LSD1/CoREST/HDAC complex, during early embryonic development.

The methylation of lysine residues within histones H3 and H4 helps to regulate the higher-order structure of chromatin in eukaryotic genomes. The consequences of lysine methylation on gene expression (unlike acetylation) can be either positive or negative, depending on the context of a particular lysine residue and the number of methyl moieties added (24, 27). Trimethylation of K9 on histone H3 (H3K9me3), for example, is generally associated with silenced genes and constitutive heterochromatin. In contrast, trimethylation of K4 on the same histone, H3 (H3K4me3), is associated with transcriptionally active regions. These methylated lysine residues provide the docking sites for the subsequent binding of chromatin-associated proteins with a cognate chromodomain, plant homeo domain (PHD) finger, or Tudor domain (42). Thus, the four methylated states of each specific lysine (unmodified or mono-, di-, or trimethylated) are interpreted by the association of other factors, such as the binding of HP1α to trimethyl H3 Lys9 (3, 29), which modify chromatin directly or indirectly. Lysine methylation *in vivo* is controlled by the opposing activities of lysine methyltransferases (KMTs) and lysine demethylases (KDMs). KDMs appear in two varieties: the amine oxidases, of which there are two (lysine-specific demethylase 1 [LSD1] and LSD2), and the much more numerous Jumonji domain-containing proteins (for a review, see references 9, 14, and 47).

Lysine-specific demethylase 1 [LSD1/AOF2/BHC110/KDM1A/SU(VAR)3-3], the first demethylase to be characterized (45), was found to specifically demethylate mono- and dimethylated H3K4 (H3K4me and H3K4me2, respectively), but not H3K4me3, *in vitro* (17, 33, 41, 45). Consistent with H3K4me2 (an active marker of transcription) as a substrate, LSD1 is found in cells as part of a core complex with the corepressor, CoREST, and histone deacetylase enzymes 1 and 2 (HDAC1 and -2) (19, 22, 62), which repress transcription by deacetylating histone tails. Interaction with CoREST prevents LSD1 degradation and is required for the recognition and demethylation of nucleosomal substrates (33, 48). The presence of HDAC1/2 suggests a coordinate modification of histone tails, which is supported by evidence that hypoacetylated histone H3 tails are the preferred substrate for LSD1 (15, 16, 32, 48). Other LSD1 complex members include the corepressor CtBP (46, 48), HMG domain containing protein, BRAF35 (19, 33), and BHC80, which contains a PHD finger that specifically recognizes unmodified H3K4 (30). Structural studies have shown that LSD1 interacts with CoREST via an extended helical region termed the "Tower" domain (6, 13, 60) and that the C-terminal SANT domain within CoREST facilitates the association with chromatin by interacting directly with DNA (60). In addition to these canonical functions, LSD1 was recently shown to be recruited to the NuRD complex, via interaction of the Tower domain with MTA1-3 in breast cancer cells (56). Furthermore, the association of LSD1 with the androgen receptor has been demonstrated to switch its substrate specificity from H3K4me/me2 to H3K9me/me2 (38, 57),

* Corresponding author. Mailing address: Department of Biochemistry, Henry Wellcome Building, Lancaster Road, University of Leicester, Leicester LE1 9HN, United Kingdom. Phone: 44 116 2297098. Fax: 44 116 2297018. E-mail: smc57@le.ac.uk.

† Supplemental material for this article may be found at http://mcb.asm.org/.

▽ Published ahead of print on 16 August 2010.

consistent with a role in gene activation (18). The composition of LSD1-containing complexes therefore has the potential to alter both target gene recruitment and substrate specificity.

In the few years since its identification, LSD1 has been shown to be crucial for a number of cellular processes. The LSD1 heterodimeric partner, CoREST, is a corepressor for the RE1 silencing transcription factor (REST), which represses neuronal genes in nonneuronal cells (2). Inhibition of LSD1 function causes increased expression of CoREST targets such as the acetylcholine receptor (AchR), synapsin, and sodium channels (SCN1A, SCN2A, and SCN3A) in nonneuronal cells (33, 45, 48). The regulation of hematopoietic differentiation via the growth factor-independent (Gfi) transcription factors is at least partially dependent on their interaction with the LSD1/CoREST/HDAC complex through an N-terminal SNAG domain (43). Pituitary development and the appropriate expression of pituitary specific hormones are also dependent on LSD1 in the mouse (55). Each of these roles involves a direct recruitment to target genes and the manipulation of histone substrates. In contrast, LSD1 function has been implicated in the DNA damage response by demethylating p53, which restricts the interaction of p53 with its cofactor p53BP1 (21). The maintenance DNA methyltransferase, Dnmt1, is another nonhistone substrate (54). Methylation of Dnmt1 by Set7/9 increases protein turnover, and therefore loss of LSD1 demethylase activity results in reduced levels of Dnmt1 and global DNA methylation. Genetic ablation of LSD1 causes early embryonic lethality at approximately embryonic day 6.5 (e6.5) (54, 55). To define a molecular mechanism for the essential embryonic role of LSD1, we have generated loss-of-function *Lsd1* gene trap mice and conditional knockout embryonic stem (ES) cells. LSD1 expression is restricted to the embryonic portion (epiblast) of the postimplantation embryo, with little or no expression in extraembryonic tissue. Loss of LSD1 in ES cells, cells equivalent to the developing primitive ectoderm of the epiblast, reveals a reduction in CoREST levels and the aberrant transcription of 588 genes, including precocious expression of genes coding for brachyury, Hoxb7, and Hoxd8, transcription factors with roles in tissue specification and limb development. Thus, the role of LSD1 is to coordinate gene expression as a key catalytic and structural component of the LSD1/CoREST/HDAC complex in early embryonic development.

MATERIALS AND METHODS

Generation of LSD1 knockout mice. An E14 mouse embryonic stem (ES) cell line containing a gene trap construct in the *Lsd1* gene locus (clone X102) was obtained from the Sanger Institute Gene Trap Resource (SIGTR) (49). The exact insertion point was determined by performing genomic PCR on these cells using gene trap and *Lsd1*-specific primers to first amplify the region and then sequence it directly. The gene trap vector, which consists of a splice acceptor site linked to a β-geo selectable marker, was found to be inserted into the 3rd intron of the *Lsd1* gene on chromosome 4. We were thus able to design primers to distinguish wild-type and mutant alleles using genomic PCR. The $Lsd1^{+/\beta\text{-geo}}$ ES cells were used to generate heterozygous mice, using standard methodology. $Lsd1^{+/\beta\text{-geo}}$ mice are viable and fertile and show no obvious adverse effects of a single mutant *Lsd1* allele. Mouse work was performed under the appropriate Home Office project license.

Generation of LSD1 knockout ES cell lines and ES cell culture. An E14 embryonic stem (ES) cell line expressing a Cre-estrogen receptor fusion protein from the *ROSA26* locus (11) was used to generate $Lsd1^{Lox/\Delta 3;\ CreER}$ cells by sequential gene targeting using an "*Lsd1cKO-Hyg*" hygromycin-resistant targeting vector. The first allele was targeted to create $Lsd1^{+/Lox}$ cells, in which exon 3 of the *Lsd1* gene was flanked by LoxP sites. This allele was deleted by adding 4-hydroxytamoxifen (4-OHT) to the cells to activate Cre, generating $Lsd^{+/\Delta 3}$ cells (lacking exon 3), before using the same Lsd1cKO-Hyg targeting vector to modify the second allele and thus create $Lsd1^{Lox/\Delta 3}$ cells. Correct gene targeting was verified by Southern blotting. Details of the targeting vector, gene targeting, and Southern blot strategy are shown in Fig. 2A. ES cell lines were maintained on gelatinized plates in standard ES cell medium consisting of knockout Dulbecco's modified Eagle's medium (DMEM) (Invitrogen); 15% fetal calf serum; 1× each glutamine, penicillin, and streptomycin (Invitrogen); 100 μM β-mercaptoethanol (Sigma-Aldrich); and leukemia inhibitory factor (LIF).

Mouse embryo analysis. Embryos at the desired developmental stage were produced from timed $Lsd1^{+/\beta\text{-geo}} \times Lsd1^{+/\beta\text{-geo}}$ matings and then isolated by dissection. Gene trap embryos were stained for X-Gal (5-bromo-4-chloro-3-indolyl-β-D-galactopyranoside) expression using a commercially available kit (InvivoGen). The appearance of blue staining typically occurred between 0.5 and 2 h. When the desired staining was achieved, embryos and ES cells were washed three times with phosphate-buffered saline (PBS) before images were taken.

Southern blot analysis. Genomic DNA was harvested from ES cells to assess gene targeting at specific time points following 4-OHT treatment to monitor deletion of exon 3 (Δ3) of the *Lsd1* gene. DNA was prepared by incubating cells overnight at 55°C with cell lysis buffer (10 mM Tris, pH 7.5, 10 mM EDTA, pH 8.0, 10 mM NaCl, 0.5% SDS, 200 μg/ml proteinase K), followed by precipitation with isopropanol and two washes with 70% ethanol (EtOH). For Southern blotting, 5 μg of genomic DNA was digested overnight with the appropriate restriction enzyme, separated on a 0.8% agarose gel, transferred to a nylon membrane by capillary blotting, and then hybridized using RapidHyb (GE Life Sciences) and a [^{32}P]dCTP-labeled probe.

Growth curve, colony formation, and alkaline phosphatase assays. To assess the proliferative potential of ES cell lines, 2.5×10^4 cells were seeded in triplicate in six-well plates and then counted each day for a 5-day period. For alkaline phosphatase assays, cells were plated at 7×10^2 cells per well in six-well plates. The medium was replaced the following day, and then cells were cultured with or without LIF for 6 days. Colonies produced after 6 days were stained with a commercial alkaline phosphatase assay kit (Millipore) for stem cell identification. The number of undifferentiated colonies stained "strongly" purple was counted. Cells were then counterstained with methylene blue and then counted to calculate the total number and percentage of differentiated colonies.

Protein analysis and HDAC assays. Nuclear protein extracts were prepared from ES cells for immunoblots as follows. A total of 3×10^7 ES cells were scraped from plates in ice-cold phosphate-buffered saline (PBS) and washed twice in PBS. Cells were resuspended in 1 ml hypotonic buffer (10 mM KCl, 20 mM HEPES, pH 7.9, 1 mM EDTA, protease inhibitor cocktail, 1 mM dithiothreitol [DTT]) and incubated on ice for 20 min. Extracts were then vortexed for 10 s during addition of 50 μl 10% NP-40, and nuclei were spun down at 1,500 rpm for 5 min at 4°C. The supernatant was removed and nuclei were resuspended in 200 μl of hypertonic lysis buffer (400 mM NaCl, 20 mM HEPES, pH 7.9, 10 mM EDTA, 25% glycerol, 1 mM DTT, protease inhibitor cocktail) for direct immunoblotting. Nuclear debris was spun down at 13,000 rpm for 10 min at 4°C. Protein concentrations were quantified using a Bradford assay. Immunoblots were performed using 20 μg of nuclear extract resolved using SDS-PAGE, 4 to 12% Bis-Tris gels (Invitrogen). For immunoprecipitation (IP), an IP buffer was used to extract whole-cell protein, containing 250 mM NaCl, 10 mM HEPES, pH 7.9, 1 mM EDTA, 0.5% NP-40, and protease inhibitors. For immunoprecipitation, 100 μg of nuclear extract was incubated overnight at 4°C with antibody. Protein G-Sepharose beads (GE Life Sciences) were blocked with 1% bovine serum albumin (BSA) in PBS. The following day, the beads and immune complexes were combined for 4 h at 4°C. After 3 washes in IP buffer, beads were split into two aliquots. One aliquot was used to assess the HDAC activity of the immunoprecipitates, using a commercially available deacetylase assay (Active Motif); 20 μl taken from 80 μl bead suspension in assay buffer was used for each reaction in 25-μl reactions using 5 μM assay substrate. Fluorometric reactions were performed in 96-well plates and analyzed on a plate reader. The remaining aliquot was resolved by SDS-PAGE and probed with antibodies raised against known components of the immunoprecipitated complexes. Antibodies to the following proteins were used: HDAC1 (Santa Cruz sc-7872; Abcam ab46985), HDAC2 (Santa Cruz sc-7899, Millipore 05-814), CoREST (Millipore 07-455), LSD1 (Sigma L4418; Abcam ab37165), mSin3a (Santa Cruz sc-767), brachyury (Sigma B8436), and β-actin (Sigma ac-74).

Histone extraction and modification analysis. Acid extraction of histones was performed as previously described (44). Five micrograms of extract was loaded in each lane, and membranes were probed using a panel of antibodies raised against a number of histone modifications. Antibodies to the following proteins were

used: H3 (Millipore 05-499), H3K9/14ac (Millipore 06-599), H3K18ac (Millipore 07-354), H3K27me3 (Millipore 07-449), H3K36ac (Millipore 07-540), H3K56ac (Active Motif 39281), H3K4me1 (Sigma M4819), H3K4me2 (Sigma D5692), and H3K4me3 (Millipore 07-473). Membranes were scanned using the Odyssey infrared imaging system, and quantification of proteins was achieved using the appropriate IRDye-conjugated secondary antibodies (LiCOR Biosciences, Cambridge, United Kingdom). The intensity of the histone modification signal was normalized to the total histone H3 loaded. Analysis was performed using three individual clones.

RNA isolation and microarray analysis. Total RNA was isolated from ES cells and embryos using a standard Trizol (Invitrogen) protocol and Phase Lock gel heavy tubes (5 Prime, Hamburg, GmbH, Germany). Microarray gene expression profiling of ES cells was performed using the Illumina mouseWG-6 v2 expression BeadChip platform. Global transcript levels in $Lsd1^{Lox/\Delta 3}$ cells and $Lsd1^{\Delta 3/\Delta 3}$ cells 10 days after addition of 4-OHT were compared. mRNA was derived from three individual ES cell clones isolated by single-cell cloning. Labeling of mRNA and hybridization were performed using a standard Illumina protocol. Statistical analysis for microarray data was performed using ArrayTrack, bioinformatics software developed by the USFDA. Raw gene expression data obtained from Illumina Bead Studio were imported to ArrayTrack; the data were then normalized using a median scaling normalization method, and $Lsd1^{Lox/\Delta 3}$ versus $Lsd1^{\Delta 3/\Delta 3}$ data sets were compared using a Welch *t* test. Significantly expressed genes were selected using cutoffs at $P < 0.05$ and a fold change of >1.4.

RT and qRT-PCR. Total RNA was reverse transcribed (RT) using Q-Script one step Supermix (Quanta Biosciences, Gaithersburg, MD). For quantitative RT-PCR (qRT-PCR), cDNA from RT reaction mixtures was diluted with an equal amount of diethyl pyrocarbonate (DEPC)-treated H_2O. Multiplex assays were designed using the Universal ProbeLibrary Assay Design Centre (www.roche-applied-science.com); primer sequences are available upon request. For each reaction, 2 μl of diluted cDNA was used in all subsequent multiplex qRT-PCRs using the Light Cycler probes master mix (Roche) as per the manufacturer's instructions. Reactions were carried out on a Roche Light Cycler 480 under the following conditions: initial denaturation for 10 min at 94°C, followed by 40 cycles of 10 s at 94°C, 20 s at 55°C, and 5 s at 72°C.

In vitro differentiation analysis. Embryoid bodies (EBs) were created by suspending 600 cells in 15-μl hanging drops in 15-cm tissue culture dishes for 48 h. Cell aggregates were collected in PBS and transferred to low-adherence 15-cm petri dishes. Plates were maintained in the CO_2 incubator on a shaking platform to allow the development of EBs. RNA was harvested from EBs at specific time points by homogenization in Trizol and chloroform phase separation in Phase Lock gel heavy tubes. Cellular RNA was precipitated using isopropanol and a glycogen carrier. EBs from each dish of hanging drops were counted at 5 days after transfer from hanging drops to petri dishes.

ChIP. Chromatin immunoprecipitation (ChIP) assays were performed as described previously (4). Briefly, 3×10^6 cells per sample were double cross-linked with 1.5 mM EGS for 20 min followed by 1% formaldehyde for 15 min (63). Cross-linking was neutralized with 0.125 M glycine, and cells were scraped in PBS. Chromatin was sonicated using the Diagenode Bioruptor for 15 min with 30-s pulse/pause cycles in polycarbonate tubes on ice to shear chromatin to 300- to 600-bp fragments. Unsheared debris was spun down, and then the chromatin was incubated overnight with the appropriate antisera, concurrent with the blocking of protein G-Sepharose beads using 2.5% BSA. Immune complexes were then precipitated using "blocked" protein G beads for 4 h at 4°C, washed three times, and then eluted. Immunoprecipitated DNA was purified and quantitative PCR was performed with 1 μl of DNA to assess LSD1 binding and histone methylation levels. The following antibodies were used: anti-LSD1 (Abcam ab37165) and anti-H3K4me2 (Sigma D5692). The following primers were used: Brachyury −4500 forward, GCTTGCTCAGTGGTTAA GGC, and reverse, GAGGTGGAGTTACAGGCAGC; Brachyury −600, forward, AGGGTCGCTATCTGTTCGTCT, and reverse, ACTGCCACTAACT CCCACCTC; and Brachyury +400, forward, GAGCATCTTTTCTTCCCA ACC, and reverse, GAAAGTTCCCGAGAAACCAAG.

Microarray data accession number. Raw data files have been deposited in the Gene Expression Omnibus (GEO) database at the NCBI (GEO accession no. GSE21131).

RESULTS

LSD1 has an essential role in the development of the embryonic epiblast. We generated mice with a gene trap insertion in the 3rd intron of the *Lsd1* gene (Fig. 1A; $Lsd1^{\beta\text{-geo}}$), which truncates the open reading frame within the SWIRM domain (Fig. 1B), prior to the amine oxidase domain, which is essential for catalytic activity. Intercrosses between $Lsd1^{+/\beta\text{-geo}}$ mice produced only wild-type and heterozygous animals, but not homozygous $Lsd1^{\beta\text{-geo}/\beta\text{-geo}}$ pups (Fig. 1C), indicating an embryonic lethal phenotype, consistent with previous reports (54, 55). We were first able to isolate homozygous $Lsd1^{\beta\text{-geo}/\beta\text{-geo}}$ embryos at embryonic day 6.5 (e6.5), which were much reduced in size compared to $Lsd1^{+/\beta\text{-geo}}$ controls (Fig. 1G), suggesting a developmental block. The introduction of the β-galactosidase open reading frame into the endogenous *Lsd1* locus allows an approximation of LSD1 protein expression patterns in cells and embryos, using X-Gal staining. The expression of LSD1 in e10.5 and e8.5 embryos was essentially ubiquitous (Fig. 1D and E). Surprisingly, X-Gal staining of early postimplantation embryos (egg-cylinder stage) revealed that LSD1 expression was restricted to the embryonic portion of the embryo, with little if any expression in the extraembryonic tissue (Fig. 1F and G). Based on this expression pattern and the developmental block in $Lsd1^{\beta\text{-geo}/\beta\text{-geo}}$ embryos at or before day e6.5, it seems that the essential embryonic role of LSD1 is restricted to cells of the developing epiblast. LSD1 is also expressed in the inner cell mass at the blastocyst stage, consistent with gene trap selection in ES cells (Fig. 1I and J). The reduced size of $Lsd1^{\beta\text{-geo}/\beta\text{-geo}}$ e6.5 embryos, a period of rapid proliferation within the epiblast (51), suggested that cells lacking LSD1 may have reduced proliferative potential. To test this hypothesis, we isolated wild-type (WT), $Lsd1^{+/\beta\text{-geo}}$, and $Lsd1^{\beta\text{-geo}/\beta\text{-geo}}$ blastocysts, plated them on gelatin-coated plates, and cultured them under standard ES cell culture conditions for 6 days. The blastocyst outgrowths from wild-type, heterozygous, and homozygous embryos all produced a similar expansion of inner cell mass cells (compare Fig. 1K, L, and M), implying that loss of LSD1 does not cause a significant reduction in proliferation. Loss-of-function experiments therefore suggest that LSD1 has an essential developmental role in the embryonic epiblast and that lethality is not caused by a general defect in cell cycle progression.

Generation and characterization of $Lsd1^{Lox/\Delta 3;\ CreER}$ ES cells. To address the molecular mechanism underlying the essential requirement for LSD1 during early embryogenesis, we generated an embryonic stem (ES) cell line in which *Lsd1* can be inactivated conditionally. Mouse ES cells are the *in vitro* counterpart of epiblast cells of the early postimplantation embryo, and their differentiation mimics many of the changes in gene expression associated with embryonic development (50). Beginning with an E14 ES cell line expressing an inducible Cre-ER fusion protein from the endogenous ROSA26 locus (11), we used sequential gene targeting to produce $Lsd1^{Lox/\Delta 3}$ cells, in which one *Lsd1* allele has exon 3 flanked by LoxP sites (floxed) and the second has exon 3 deleted (Fig. 2A). Induction of Cre activity by addition of 4-hydroxytamoxifen (4-OHT) to the growth medium resulted in complete recombination of the remaining floxed allele (to generate $Lsd1^{\Delta 3/\Delta 3}$) within 6 h (Fig. 2B). Loss of exon 3 disrupts the open reading frame of LSD1 such that a premature stop codon is introduced into exon 4, resulting in the progressive loss of LSD1 protein (Fig. 2C and D) and mRNA, presumably due to nonsense-mediated decay (Fig. 2E). Loss of LSD1 protein did not change the proliferative potential (Fig. 2F) or cell cycle profile (Fig. 2G) of ES cells, consistent with the embryo outgrowth phenotype

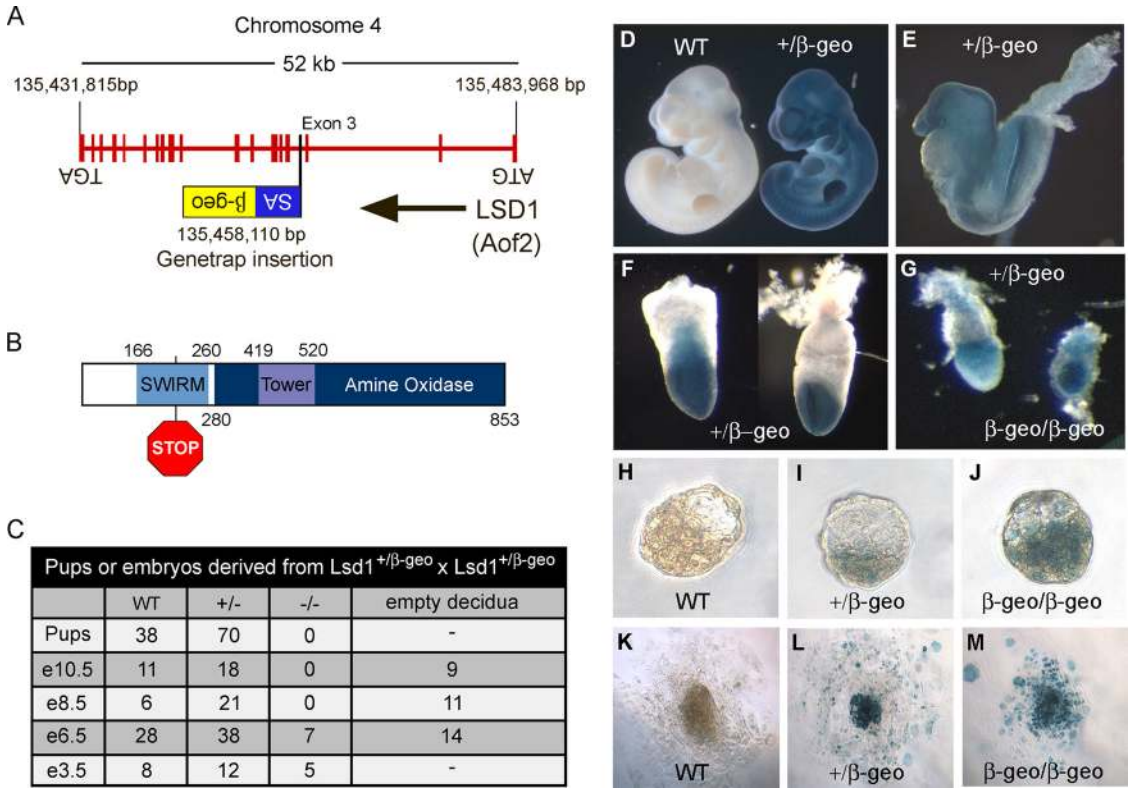

Pups or embryos derived from Lsd1$^{+/\beta\text{-geo}}$ x Lsd1$^{+/\beta\text{-geo}}$

	WT	+/-	-/-	empty decidua
Pups	38	70	0	-
e10.5	11	18	0	9
e8.5	6	21	0	11
e6.5	28	38	7	14
e3.5	8	12	5	-

FIG. 1. A gene trap insertion inactivates *Lsd1* and reveals embryo-specific expression. (A) A mouse embryonic stem (ES) cell line containing a gene trap vector in the *Lsd1* gene locus (clone X102) was used to generate *Lsd1*$^{+/\beta\text{-geo}}$ mice. The gene trap vector, which consists of a splice acceptor site linked to a β-geo selectable marker, was found to be inserted into the 3rd intron of the *Lsd1* gene on chromosome 4. (B) Schematic representation of LSD1. The position of the gene trap insertion (STOP), downstream of exon 3, truncates the LSD1 open reading frame within the SWIRM domain prior to the amine oxidase domain, which is essential for the catalytic activity of LSD1. Numbers indicate the positions of specific amino acids of the SWIRM, Tower, and amine oxidase domains. (C) The table shows the numbers and genotypes of viable pups and embryos isolated. Numbers of empty decidua are also listed. (D) Wild-type and *Lsd1*$^{+/\beta\text{-geo}}$ embryos isolated at 10.5 days postcoitum (dpc) were stained with X-Gal to detect β-galactosidase reporter gene activity approximating to LSD1 expression patterns. Similar X-Gal staining experiments were performed using embryos isolated at 8.5 dpc (E), 8.0 dpc (F), 6.5 dpc (G), and 3.5 dpc (H to J). The genotype of individual embryos is indicated. (K to M) X-Gal staining of blastocyst outgrowth cultures shows wild-type, *Lsd1*$^{+/\beta\text{-geo}}$, and *Lsd1*$^{\beta\text{-geo}/\beta\text{-geo}}$ cells that were isolated at 3.5 dpc and cultured on gelatinized plates for 6 days. On day 6, blastocyst outgrowth cultures were stained with X-Gal to determine β-galactosidase expression and then genotyped.

(Fig. 1K to M). In subsequent experiments, *Lsd1*$^{Lox/\Delta 3;\ CreER}$ cells (henceforward referred to as *Lsd1*$^{Lox/\Delta 3}$) were compared to *Lsd1*$^{\Delta 3/\Delta 3}$ cells, 7 to 14 days after 4-OHT treatment. Importantly, global DNA methylation levels are comparable to control cells during this time period, as measured by the incomplete digestion of endogenous retroviral element (specifically IAP) using a methylation-sensitive (HpaII) restriction enzyme (Fig. 2H, left panel), whereas continued culture of ES cells lacking LSD1 (>25 days) (Fig. 2H) results in decreased global DNA methylation, consistent with the results of Wang and colleagues (54).

Loss of LSD1 causes a reduction in the level of CoREST protein and increased histone acetylation. The corepressor, CoREST, is a central binding partner of LSD1 in cells and together with histone deacetylases 1 and 2 (HDAC1 and -2) forms an LSD1/CoREST/HDAC core complex (19, 32, 33, 48, 62). To test the integrity of the remaining complex in the absence of LSD1, we purified CoREST from *Lsd1*$^{\Delta 3/\Delta 3}$ cells and tested its ability to interact with HDAC1 and -2. In *Lsd1*$^{Lox/\Delta 3}$ control cells, CoREST copurifies with LSD1, HDAC1, and HDAC2 (Fig. 3A, lane 5). In the absence of LSD1, we observe a decrease in the level of CoREST protein (Fig. 3A, compare lanes 1 and 6, and 3B), suggesting a codependence for protein stability since CoREST mRNA is unaffected (Fig. 3C). The reduction in CoREST correlates with a decrease in the association of HDAC1 and -2 proteins (Fig. 3A, compare lanes 5 and 10) and deacetylase activity (Fig. 3D). However, although the association is reduced, we can still monitor a physical and biochemical association of CoREST with HDACs, suggesting that this portion of the complex is still intact. As a control, the association of HDAC1 with a distinct corepressor protein, Sin3A, was tested and found to be unaffected by loss of LSD1 (Fig. 3A). Nor was there a change in the overall activity of HDAC1 in *Lsd1*$^{\Delta 3/\Delta 3}$ cells (Fig. 3D).

A reduction in the deacetylase activity of the CoREST complex in the absence of LSD1 and the observation that LSD1 preferentially demethylates mono- and dimethylated histone H3 K4 (H3K4me1/me2) (15, 16, 48) prompted us to examine the posttranslational modification of histone H3 in *Lsd1*$^{\Delta 3/\Delta 3}$ cells. Loss of LSD1 produced only a small increase in the

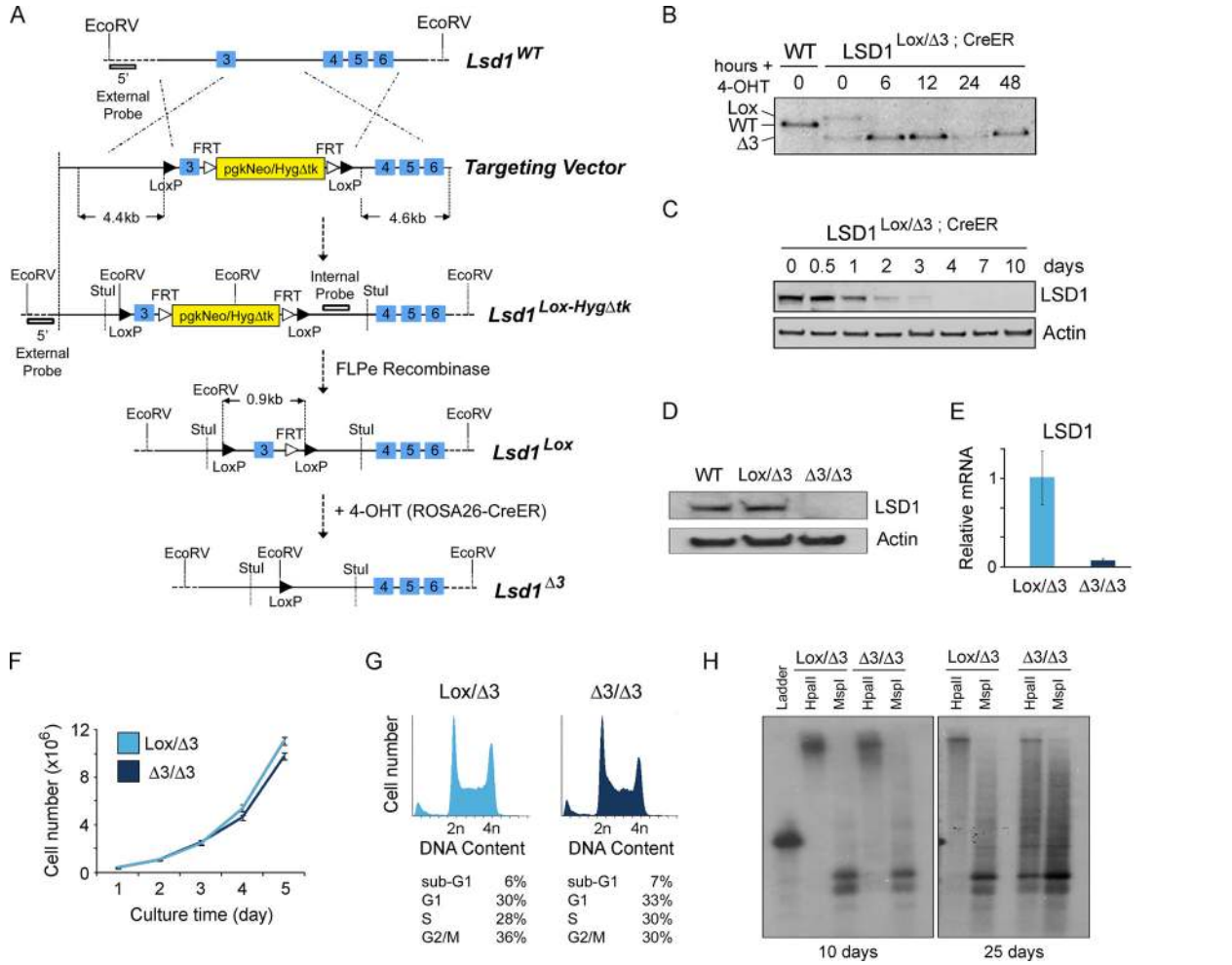

FIG. 2. Generation of a conditional LSD1 knockout ES cell line. (A) E14 ES cells expressing a Cre/estrogen receptor fusion protein from the *ROSA26* locus (11) were used to produce a 4-hydroxy tamoxifen (4-OHT)-inducible, conditional knockout (cKO) system. Exon 3 of the *Lsd1* gene was flanked by LoxP sites (floxed) using an "*Lsd1cKO-Hyg*" gene targeting vector. The sizes of homology arms and positions of LoxP (black triangle) and FRT (white triangle) sites are indicated. Correct gene targeting was assessed by Southern blotting using a 5′ external probe following an EcoRV digest. Correctly targeted $Lsd1^{+/Lox\text{-}Hyg\Delta TK}$ cells were treated with 4-OHT for 6 h to induce LoxP recombination and generate $Lsd1^{+/\Delta 3}$ cells. Successfully recombined cells were identified by Southern blotting using an internal probe and StuI digest. The second, wild-type, allele of $Lsd1^{+/\Delta 3}$ cells was targeted with the *Lsd1cKO-Hyg* targeting vector again to produce $Lsd1^{Lox\text{-}Hyg\Delta TK/\Delta 3}$ cells. Transient transfection of $Lsd1^{Lox\text{-}Hyg\Delta TK/\Delta 3}$ cells with FLPe recombinase was used to remove the selection cassette and produce $Lsd1^{Lox/\Delta 3}$ cells used in the study. (B) Southern blot showing wild-type bands, LoxP-targeted bands (Lox), and bands with exon 3 deleted (Δ3). Addition of 4-OHT activates the CreER fusion protein and induces deletion of exon 3 within 6 h, generating a frameshift and introduction of a premature stop codon in exon 4 (C) The Western blot shows ligand-inducible deletion of LSD1 protein in nuclear extracts from $Lsd1^{Lox/\Delta 3}$ ES cells. Cells were cultured for up to 10 days (0 to 2 days in the presence of 4-OHT). β-Actin was used to normalize for protein loading. (D) The Western blot shows that LSD1 protein levels are equivalent in wild-type and heterozygous ($Lsd1^{Lox/\Delta 3}$) ES cells. $Lsd1^{Lox/\Delta 3}$ cells are used as a control throughout the study. (E) Quantitative RT-PCR reveals a decrease in LSD1 mRNA levels due to nonsense-mediated decay following exon 3 deletion. (F) The growth rate of the indicated cells was assessed by counting cells over a 5-day period from initial plating of 2.5×10^4 cells. (G) Propidium iodide staining and FACS analysis reveal similar cell cycle profiles of $Lsd1^{Lox/\Delta 3}$ and $Lsd1^{\Delta 3/\Delta 3}$ ES cells. The percentage of cells with a sub-G_1, 2n (G_1), S phase, or 4n (G_2/M) DNA content is indicated. (H) Southern blotting was used to assess the level of genomic methylation at intracisternal A-particle (IAP) elements. Genomic DNA from $Lsd1^{Lox/\Delta 3}$ and $Lsd1^{\Delta 3/\Delta 3}$ ES cells either 10 (left panel) or 25 days (right panel) postrecombination was digested with either HpaII (methylation sensitive) or MspI (methylation resistant) restriction enzyme and then hybridized with an IAP probe.

global levels of H3K4me1 and H3K4me2, suggesting that locus-specific changes in methylation may be occurring (Fig. 3E). Rather than significant changes in lysine methylation, we observe a 1.3-fold increase in H3K9 acetylation (H3K9Ac) and a 2-fold increase in H3K56Ac consistent with a decrease in the HDAC activity associated with CoREST. This implies that H3K56Ac, a modification associated with DNA damage (10, 53), nucleosome assembly (10), and the activity of stem cell factors (59) in higher eukaryotes, is a substrate for the CoREST complex. Taken together, it appears that LSD1 helps regulate global histone acetylation via stabilization of the LSD1/CoREST/HDAC complex in ES cells.

***Lsd1*$^{\Delta 3/\Delta 3}$ ES cells retain stem cell characteristics but have impaired differentiation.** In light of the biochemical changes in $Lsd1^{\Delta 3/\Delta 3}$ cells, we wanted to assess what affect loss of LSD1 might have on the growth characteristics of ES cells. As shown

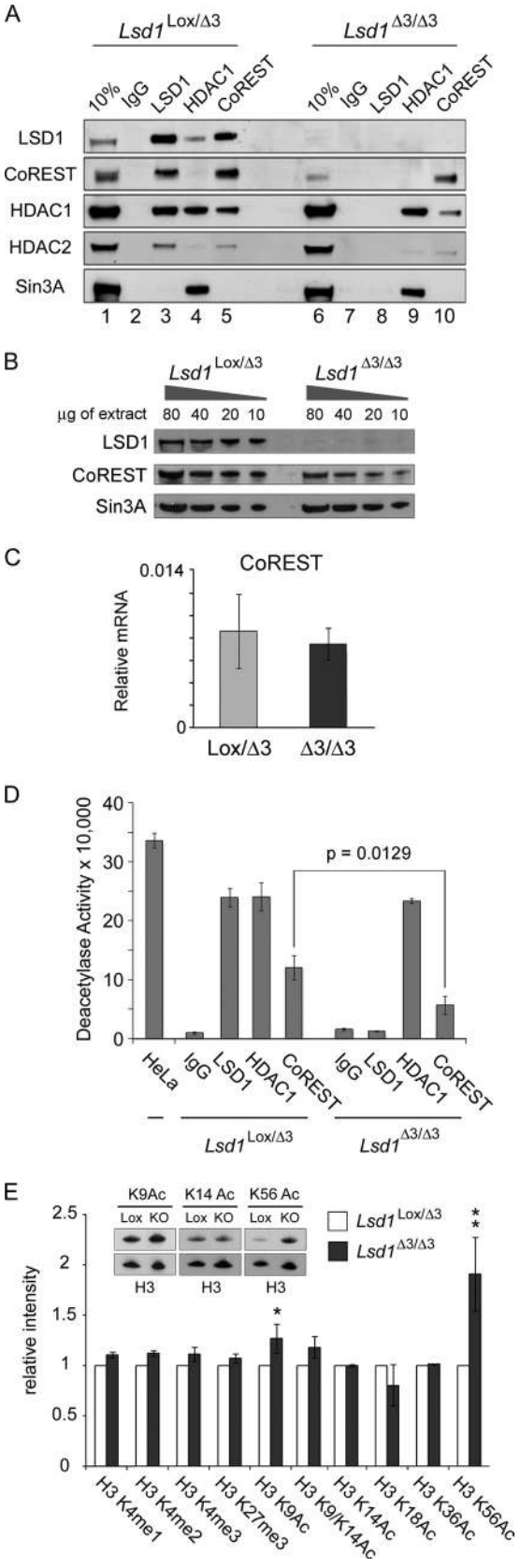

FIG. 3. Loss of LSD1 results in decreased CoREST protein levels and an increase in histone acetylation. (A) Specific antisera to the indicated proteins were used to immunoprecipitate LSD1, HDAC1, and CoREST from $Lsd1^{Lox/\Delta3}$ and $Lsd1^{\Delta3/\Delta3}$ ES cells. Normal rabbit IgG was used as a control. Coimmunoprecipitated proteins were assessed by immunoblotting for the proteins indicated. (B) Western blotting using the indicated amounts of nuclear extract from $Lsd1^{Lox/\Delta3}$ and $Lsd1^{\Delta3/\Delta3}$ ES cells reveals a reduction in CoREST protein in the absence of LSD1. Sin3A was used as a loading control. (C) Quantitative RT-PCR reveals that CoREST is not regulated by LSD1 through transcriptional control. CoREST mRNA levels, normalized to GAPDH, are similar in $Lsd1^{Lox/\Delta3}$ and $Lsd1^{\Delta3/\Delta3}$ ES cells. (D) The amount of deacetylase activity associated with each immunoprecipitation was measured using a commercially available kit. Mean values are plotted ($n = 3$) ± standard error of the mean (SEM). (E) The methylation and acetylation status of histone H3 was detected using quantitative Western blotting. Histones were acid extracted from three different $Lsd1^{Lox/\Delta3}$ and $Lsd1^{\Delta3/\Delta3}$ clones. The signal of specific modification was normalized to the total amount of H3 and quantitated using an Odyssey scanner (**, $P < 0.01$, and *, $P < 0.05$; Students t test).

previously, proliferation capacity was unperturbed by loss of LSD1 (Fig. 2F), we therefore compared the ability of $Lsd1^{Lox/\Delta3}$ and $Lsd1^{\Delta3/\Delta3}$ cells to differentiate. ES cells with and without LSD1 were plated at clonal density and cultured for a further 5 days in the presence or absence of leukemia inhibitory factor (LIF) to simulate differentiation. Cells were then stained for the presence of alkaline phosphatase (AP), a marker of pluripotency. Plating cells at clonal density measures two things: ability to retain pluripotency in the presence of LIF and the potential to differentiate without it. $Lsd1^{\Delta3/\Delta3}$ cells showed a similar percentage of differentiated colonies to $Lsd1^{Lox/\Delta3}$ controls in both the presence and absence of LIF (Fig. 4A). However, the overall number of colonies observed in the absence of LIF was reduced by approximately 60% (Fig. 4B), suggesting that differentiation may be associated with increased cell death. We observed a similar reduction in the number of embryoid bodies (EBs) derived from $Lsd1^{\Delta3/\Delta3}$ cells compared to $Lsd1^{Lox/\Delta3}$ controls after hanging-drop culture (Fig. 4C). Therefore, to address whether increased cell death was associated with differentiation in the absence of LSD1, $Lsd1^{Lox/\Delta3}$ and $Lsd1^{\Delta3/\Delta3}$ cells were cultured in the presence of retinoic acid (RA) to stimulate differentiation, and then the accumulation of cells with a sub-G_1 DNA content was measured (Fig. 4D). Prior to RA treatment, both $Lsd1^{Lox/\Delta3}$ and $Lsd1^{\Delta3/\Delta3}$ cells show only a small population of dead cells (day 0). In contrast, after 3 days of RA treatment, 58% of $Lsd1^{\Delta3/\Delta3}$ cells showed a sub-G_1 DNA content, over 2-fold more than $Lsd1^{Lox/\Delta3}$ controls. Differentiation due to the absence of LIF in the culture media produced a similar increase in the percentage of dead $Lsd1^{\Delta3/\Delta3}$ cells (data not shown). Together, these data suggest that cells lacking LSD1 are susceptible to cell death upon differentiation. Continued culture of the surviving EBs lacking LSD1 revealed that they still retain the ability to switch off the pluripotent factors Oct-4, Nanog, and Rex-1 (Fig. 4E), despite disruption of the LSD1/CoREST/HDAC complex. Differentiation into the three primary germ layers was also initiated since we observe the activation of markers for primitive ectoderm (FGF5), mesoderm (brachyury), and endoderm (Gata6). The level of brachyury

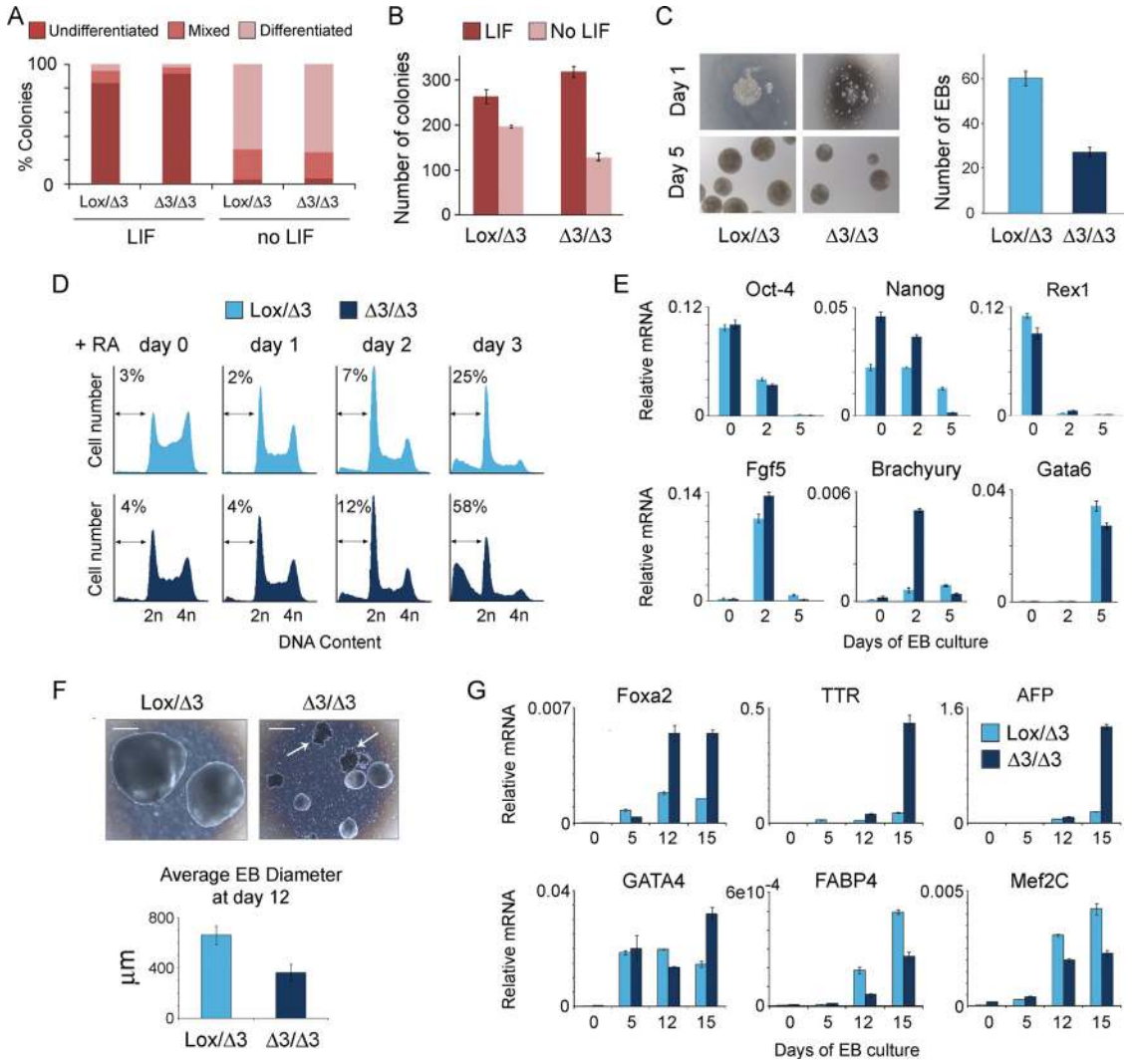

FIG. 4. Differentiation of ES cells lacking LSD1 is associated with increased cell death and a perturbed transcriptional program. (A) Differentiation potential. ES cells of the indicated genotype were plated at low density in the presence or absence of LIF and cultured for 6 days before staining for the presence of alkaline phosphatase and scored as undifferentiated (intense purple), mixed (weak purple), or differentiated (no staining). (B) Colonies were stained with methylene blue and counted. Mean values are plotted ($n = 3$) ± SEM. (C) The left panel shows images representative of embryoid bodies (EBs) at 1 and 5 days of culture, and the right panel shows the number of EBs of the indicated genotype obtained after 5 days of culture. (D) The percentage of dead cells was determined by propidium iodide staining and FACS analysis, after treatment with 1 μM retinoic acid. The percentage of cells with a sub-G_1 DNA content is indicated. (E) Quantitative RT-PCR data for genes characteristic of undifferentiated stem cells (Oct-4, Nanog, and Rex1), endoderm (Gata6), primitive ectoderm (Fgf5), and mesoderm (brachyury), was performed as indicated on mRNA collected at days 0, 2, and 5 during EB differentiation. Mean values ($n = 3$) ± SEM are plotted. Values indicate expression of the specific gene relative to GAPDH measured using Universal ProbeLibrary hydrolysis probes. (F) Representative bright-field image (top panel) and average size of EBs (bottom panel) after 12 days of culture. Arrows indicate clumps of dead cells which accumulate in *Lsd1*$^{\Delta 3/\Delta 3}$ cultures. Scale bar = 300 μm. The bottom panel shows the diameter of EBs of the indicated genotype obtained after 12 days of culture. (G) Quantitative RT-PCR was performed as in panel E for markers of endoderm (TTR, AFP, and Foxa2), adipose (FABP4), and cardiomyocyte (Mef2c) tissue. mRNA was isolated from EBs of the indicated genotype at 0, 5, 12, and 15 days of culture.

mRNA was notably higher in both cycling ES cells and day 2 EBs lacking LSD1, indicating an altered pattern of gene transcription which could potentially perturb differentiation. Extended culture over a period of 15 days revealed that EBs derived from *Lsd1*$^{\Delta 3/\Delta 3}$ cells were approximately half the size of controls (Fig. 4F) and had an enrichment of endodermal cell types (Fig. 4G; increased Foxa2, TTR, and AFP expression). However, given the abnormal size and morphology of EBs with LSD1 deleted, this enrichment may represent the absence of other cell types due to increased cell death. Overall, it appears that ES cells lacking LSD1 proliferate normally under standard ES cell culture conditions and retain stem cell characteristics (AP, Oct-4, and Nanog expression) but show increased levels of cell death upon differentiation, which may be related to an aberrant transcriptional program.

LSD1 regulates the ES cell transcriptome. To examine the consequence of LSD1 deletion on the ES cell transcriptome,

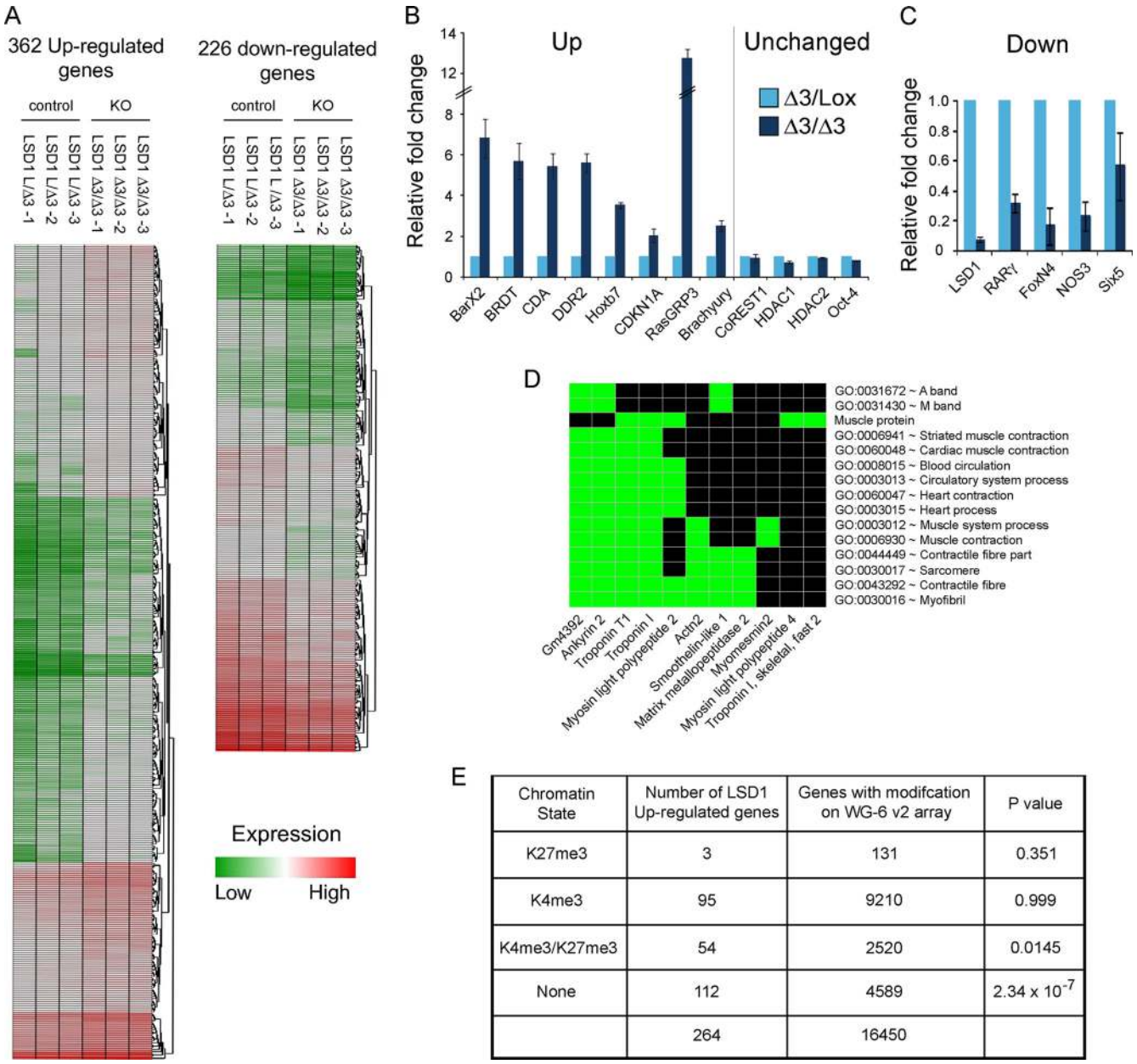

E

Chromatin State	Number of LSD1 Up-regulated genes	Genes with modifcation on WG-6 v2 array	P value
K27me3	3	131	0.351
K4me3	95	9210	0.999
K4me3/K27me3	54	2520	0.0145
None	112	4589	2.34×10^{-7}
	264	16450	

FIG. 5. Loss of LSD1 results in the aberrant expression of 588 genes greater than 1.4-fold. (A) A heat map shows up- and downregulation of genes altered by >1.4-fold, clustered by similarity in expression profile, between $Lsd1^{Lox/\Delta 3}$ and $Lsd1^{\Delta 3/\Delta 3}$ cells. Experiments were performed in triplicate using mRNA from three individual ES cell clones. (B) Quantitative RT-PCR validation of transcripts upregulated in $Lsd1^{\Delta 3/\Delta 3}$ cells and unchanged control genes. (C) Quantitative RT-PCR validation of transcripts downregulated in $Lsd1^{\Delta 3/\Delta 3}$ cells. Values are expressed relative to the level of transcript in $Lsd1^{Lox/\Delta 3}$ for panels B and C. Mean values ($n = 3$) ± SEM are plotted. (D) Functional annotation clustering of upregulated genes, using DAVID, identifies an enrichment for genes with a muscle-specific function. Gene names and associated gene ontology (GO) terms are listed. A green block indicates a corresponding gene term association positively reported. (E) Upregulated genes were subdivided by their original chromatin state in mouse ES cells. Genes were classified by the presence of either trimethylated histone H3 Lys4 (K4me3), Lys27 (K27me3), both Lys4 and Lys27 (K4me3/K27me3), or neither modification (none). The number of upregulated genes, the number of genes present on the WG-6 v2 array with a particular modification, and the enrichment of genes with one of the four potential chromatin states (*P* value, calculated using a hypergeometric test) are indicated.

we isolated RNA from $Lsd1^{Lox/\Delta 3}$ and $Lsd1^{\Delta 3/\Delta 3}$ cells to perform a comparative microarray analysis using an Illumina BeadChip platform, which covers 45,200 different mouse transcripts. Transcripts which were up- or downregulated by greater than 1.4-fold ($P < 0.05$) across three independent experiments, each using a separate ES cell clone, were identified using ArrayTrack analysis software (see Materials and Methods). In total, 588 transcripts were differentially regulated, the majority of which were upregulated (362 upregulated compared with 226 downregulated), consistent with a role for LSD1 in transcriptional repression (Fig. 5A; for a complete list, see Table S1 in the supplemental material). Brachyury,

which we identified previously as being upregulated in cells with LSD1 deleted (Fig. 4E) was increased 1.4-fold, while LSD1 itself was the transcript reduced most (3-fold down), thus providing useful internal controls for the experimental system. To further verify the microarray results, we quantified the levels of eight upregulated, five downregulated, and four unchanged transcripts by qRT-PCR (Fig. 5B and C). In each instance (17/17 transcripts), we were able to corroborate the microarray result. Indeed, for many genes we observe a more robust change in transcript levels by qRT-PCR (e.g., Brdt 1.9-fold upregulation by microarray compared to 5.5-fold upregulation by qRT-PCR). Of particular interest were genes with a role in embryonic development whose aberrant expression might relate to the embryonic lethal phenotype of the *Lsd1*$^{\beta\text{-geo}/\beta\text{-geo}}$ embryos. We identified a number of transcription factors with functions in tissue specification and limb development, including, brachyury, Gli2, and RARγ and a number of homeobox-containing proteins: Hoxb7, Hoxd8, and Barx2. An analysis of functionally related gene groups among our upregulated gene list using DAVID (20), revealed an enrichment for genes involved in cardiac and striated muscle contraction (Fig. 5D). This suggests that LSD1 may regulate mesodermal differentiation, which correlates well with increased levels of brachyury, a master regulator of mesoderm specification in the developing embryo. Thus, an altered transcriptional program, including precocious expression of muscle-specific factors, may contribute to the impaired developmental phenotype of LSD1 knockout embryos and cells.

Gene expression is tightly linked with histone modifications such as H3K4me3 and H3K27me3, which have a positive and negative association, respectively, with transcription. In ES cells, many genes with a lineage-specific function retain both H3K4me3 and H3K27me3 modifications and are deemed to be bivalent (1, 5, 39). As a regulator of H3K4 methylation, we were interested in determining the initial chromatin state of genes altered by loss of LSD1. Using available histone modification data sets for mouse ES cells (28, 39), genes upregulated in the absence of LSD1 were subdivided into four classes based on their methylation status at H3K4 and H3K27 (Fig. 5E; see Table S2 in the supplemental material). We observed a significant enrichment for bivalent genes ($P = 0.0145$) among upregulated transcripts and an even higher association of genes without either H3K4me3 or H3K27me3 modifications ($P = 2.34 \times 10^{-7}$). Downregulated genes by definition must be initially active and therefore show a very high association with H3K4me3, but not H3K27me3 or H3K4me3/H3K27me3, which is a useful control but not informative (data not shown). Thus, it appears that LSD1 plays a role in the transcriptional balance of bivalently modified genes, but preferentially controls those without either H3K4me3 or H3K27me3 chromatin marks.

***brachyury* is a direct LSD1 target gene and is upregulated in e6.5 *Lsd1*$^{\beta\text{-geo}/\beta\text{-geo}}$ embryos.** A correlation between LSD1 loss, increased brachyury expression, and the activation of mesodermal, notably, muscle-specific genes, prompted us to investigate the relationship between LSD1 and brachyury further. We examined brachyury expression in *Lsd1*$^{Lox/\Delta 3}$ and *Lsd1*$^{\Delta 3/\Delta 3}$ cells either with or without LIF to stimulate ES cell differentiation. LIF withdrawal leads to an increase in brachyury mRNA levels in both control cells and cells with LSD1 deleted, although expression is still higher in the absence of LSD1 (Fig. 6A). Brachyury protein levels are similarly increased by the absence of LSD1 in differentiated and undifferentiated ES cells (Fig. 6B). Both results confirmed that LSD1 negatively regulates brachyury expression. We therefore wanted to test if this was a consequence of direct recruitment of LSD1 to the *brachyury* gene. Using chromatin immunoprecipitation (ChIP), we could show that LSD1 is associated with the *brachyury*

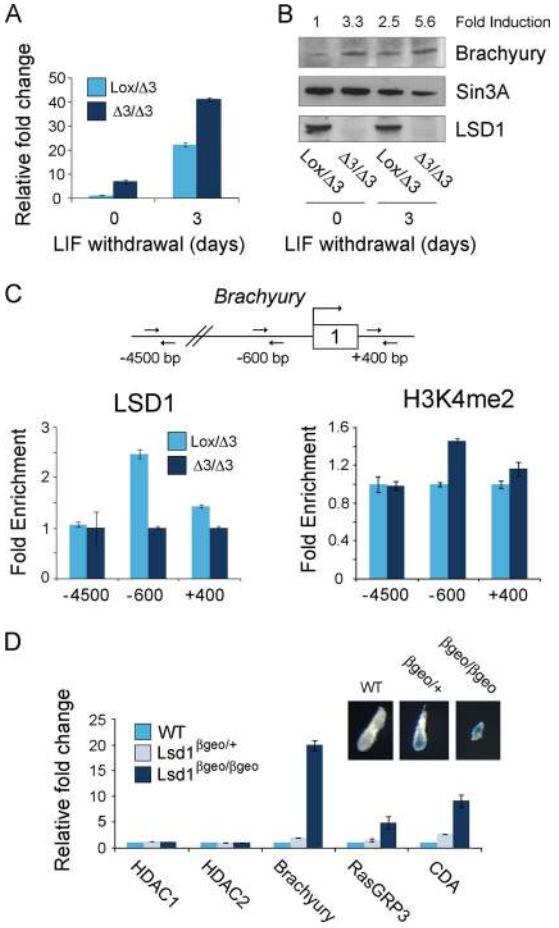

FIG. 6. *brachyury*, a direct target gene of LSD1, is derepressed in *Lsd1*$^{\beta\text{-geo}/\beta\text{-geo}}$ gene trap embryos. (A) Quantitative RT-PCR shows upregulation of brachyury mRNA in *Lsd1*$^{\Delta 3/\Delta 3}$ ES cells, with (day 0) and without (day 3) LIF. Values are expressed relative to the level of transcript in *Lsd1*$^{Lox/\Delta 3}$ cells with LIF. (B) The Western blot shows an increase in brachyury protein levels in *Lsd1*$^{\Delta 3/\Delta 3}$ ES cells with (day 0) and without (day 3) LIF. The fold induction of brachyury protein was calculated relative to Sin3A. (C) A schematic of the *brachyury* gene shows relative position of primers used for quantitative PCR following chromatin immunoprecipitation (ChIP). A region −600 bp from the transcriptional start site is enriched in anti-LSD1 ChIPs from *Lsd1*$^{Lox/\Delta 3}$ but not *Lsd1*$^{\Delta 3/\Delta 3}$ cells, showing specific enrichment of LSD1 protein (left panel). Loss of LSD1 protein results in increased histone H3 K4 dimethylation at the −600-bp region (right panel). (D) Quantitative RT-PCR analysis of e6.5 embryos. Homozygous (*Lsd1*$^{\beta\text{-geo}/\beta\text{-geo}}$) embryos have a 20-fold increase in brachyury mRNA compared with wild-type and heterozygous (*Lsd1*$^{+/\beta\text{-geo}}$) embryos. RasGRP3 transcription (5-fold) and CDA transcription (10-fold) are similarly increased in *Lsd1*$^{\beta\text{-geo}/\beta\text{-geo}}$ embryos. Assays were performed in triplicate with individual embryos of each genotype. Values are expressed relative to the level of transcript in wild-type embryos; mean values ($n = 3$) ± SEM are plotted.

promoter region, with a maximal enrichment (2.4-fold) approximately 600 bp upstream of the transcriptional start site (Fig. 6C). Reduced LSD1 binding could be detected downstream of the first exon (+400 bp), with no association detected with more distal 5′ regions (−4,500 bp) of the brachyury locus. This binding was specific since we fail to observe any enrichment in *Lsd1*$^{\Delta 3/\Delta 3}$ cells lacking LSD1 protein. In the absence of LSD1, we were also able to detect a subtle (1.4-fold) increase in the level of H3K4me2 centered around the −600-bp region, indicative of increased transcription and the loss of LSD1 enzymatic activity. Finally, we wanted to relate the increase in brachyury expression observed in *Lsd1*$^{\Delta 3/\Delta 3}$ ES cells back to *Lsd1*$^{\beta\text{-geo}/\beta\text{-geo}}$ embryos *in vivo*. Wild-type, *Lsd1*$^{+/\beta\text{-geo}}$, and *Lsd1*$^{\beta\text{-geo}/\beta\text{-geo}}$ e6.5 embryos were isolated, and the whole embryo was used for RNA extraction, followed by cDNA synthesis and qRT-PCR. As a control, we tested the expression of HDAC1 and HDAC2, whose mRNA and protein levels were unchanged by loss of LSD1 (Fig. 3A and 5B), and found that their expression was not altered between embryos with LSD1 deleted and controls (Fig. 6D). In contrast, brachyury expression was increased significantly in *Lsd1*$^{\beta\text{-geo}/\beta\text{-geo}}$ embryos compared to *Lsd1*$^{+/\beta\text{-geo}}$ heterozygous controls. The genes coding for RasGRP3 and CDA, two genes upregulated in *Lsd1*$^{\Delta 3/\Delta 3}$ ES cells, are similarly upregulated in *Lsd1*$^{\beta\text{-geo}/\beta\text{-geo}}$ embryos, demonstrating a consistent relationship between the two systems. These data infer that LSD1 is recruited directly to the *brachyury* locus in order to restrict its expression prior to differentiation in ES cells and gastrulation in the developing embryo.

DISCUSSION

LSD1 is essential for survival of the postimplantation embryo. We have shown that embryos with a homozygous gene trap insertion in the *Lsd1* locus (*Lsd1*$^{\beta\text{-geo}/\beta\text{-geo}}$) die at around e6.5, consistent with previous reports (54, 55). *Lsd1*$^{\beta\text{-geo}/\beta\text{-geo}}$ embryos are reduced in size compared to heterozygous controls (Fig. 1G), suggesting a block to development shortly after implantation. Unlike the ubiquitous expression pattern observed at the head-fold stage and beyond (Fig. 1D and E), LSD1 expression in the postimplantation embryo is restricted to the embryonic portion of the embryo (Fig. 1F and G). Based on this expression pattern, it appears that *Lsd1*$^{\beta\text{-geo}/\beta\text{-geo}}$ embryos lack extraembryonic tissue, suggesting that development stalls before the elongation of the epiblast into embryonic and extraembryonic lineages (Fig. 1G) (54). Prior to implantation, *Lsd1*$^{\beta\text{-geo}/\beta\text{-geo}}$ blastocysts occurred at normal Mendelian ratios and appeared to be morphologically normal. It takes 3 to 4 days following genetic deletion for LSD1 protein to turnover (Fig. 2C), suggesting that although maternal LSD1 mRNA may drop between cell stages 2 to 16 (36), maternally derived LSD1 protein could persist until the blastocyst stage. Cultured *Lsd1*$^{\beta\text{-geo}/\beta\text{-geo}}$ blastocysts show a robust outgrowth of the inner cell mass when cultured *in vitro* (Fig. 1M), and cells with LSD1 deleted show no reduction in proliferative potential (Fig. 2F), suggesting that embryonic lethality occurs because of an aberrant developmental program, not impaired proliferation. Altered expression of key developmental regulators in ES cells lacking LSD1 supports this hypothesis (discussed below).

Multiple lysine demethylase (KDM) enzymes can demethylate mono- and dimethylated histone H3 lysine 4 (H3K4me/me2) *in vivo*. In addition to LSD1, the related amine oxidase LSD2 (KDM1B) and the Jumonji domain-containing enzymes KDM5A, KDM5B, KDM5C, and KDM5D have all been shown to demethylate H3K4me2 (7, 8, 23, 25, 26, 31, 34). All but KDM5D appear to be expressed in embryonic cells (52, 58). Mice with expression of LSD2 (8) and KDM5A (26) knocked out have been generated, but despite similar biochemical activities and substrate specificities to LSD1, neither one is required for embryonic development. Given the degree of enzymatic redundancy, the essential requirement for LSD1 implies that it may have critical substrates other than H3K4, potentially nongenomic targets such as Dnmt1 (54). Alternatively, the association with proteins such as CoREST could be indispensable. LSD2, the KDM most related to LSD1, lacks a Tower domain required for the interaction with CoREST (25). Thus, the ability to interact with CoREST and histone deacetylases 1 and 2 (HDAC1 and -2) may be a crucial dimension to LSD1 function *in vivo*.

ES cells lacking LSD1 have reduced levels of CoREST and increased histone acetylation. Conditional deletion of LSD1 from ES cells results in a reduction of CoREST protein (Fig. 3B), consistent with the demonstration that knockdown of CoREST reduces LSD1 levels (48), suggesting a codependence on protein stability. HDAC1 and -2, which occur in multiple complexes in addition to the LSD1/CoREST complex (61), were unaffected. CoREST, although reduced, is still able to associate with HDAC1/2 (Fig. 3A, lane 10), most likely via an N-terminal region containing an ELM2 domain (32) in an LSD1-independent manner. Perturbation of the LSD1/CoREST/HDAC complex causes a number of small, but reproducible changes in global histone modification. The androgen and estrogen receptors, factors which can switch LSD1 specificity from H3K4me/me2 to H3K9me/me2 (18, 38, 57), are absent from ES cells; we therefore focused on the methylation status of H3K4. H3K4me/me2 levels are increased only slightly, in accord with the results of Wang and colleagues (54). ChIP-on-chip data suggest that LSD1 is associated with a large number of gene promoters (18, 43, 56), >70% of which are positive for H3K4me3 (either univalent or bivalent with H3K27me3) (39) in ES cells; therefore, perhaps it is not surprising that H3K4me2 is relatively unchanged upon LSD1 loss. In contrast, the LSD1-dependent reduction in CoREST protein and associated HDAC1/2 results in a 1.3-fold increase in H3K9 acetylation (H3K9Ac) and a 2-fold increase in H3K56Ac, a modification associated with the DNA damage response (10, 53), histone deposition (10), and the activity of stem cell factors (59) in higher eukaryotes. The observation that H3K56Ac levels are affected more than other acetylated lysines within histone H3 is likely a reflection of their relative abundance in ES cells. The increase in H3K9/K14Ac and H4Ac levels in ES cells treated with TSA is relatively modest compared to the level in somatic cells (11), suggesting that histone tails are already in a hyperacetylated state. In contrast, only 1% of histone H3 is acetylated at K56 in ES cells (59), making small changes in K56Ac levels due to the alteration of HDAC1/2 complexes more apparent. Increased H3K56Ac correlates with reduced CoREST levels (while HDAC1/2 levels are constant), implying that H3K56Ac is regulated by the LSD1/CoREST/HDAC complex, although it remains to be

demonstrated whether this is a direct association. Thus, it appears that LSD1, a lysine demethylase, functions in part by regulating the lysine acetylation status of chromatin by stabilizing the CoREST-HDAC1/2 interaction as part of the LSD1/CoREST/HDAC core complex. The ternary complex, which is enzymatically more active than individual components (32), is then capable of functioning independently (43, 62) or as a module of broader protein complexes containing multiple chromatin-associated factors (19, 33, 46, 48).

ES cells lacking LSD1 retain stem cell characteristics and are able to initiate differentiation. Despite perturbation of the LSD1/CoREST/HDAC complex, we found that ES cells with LSD1 deleted retain stem cell characteristics (expression of Oct4, Nanog, and alkaline phosphatase) and were still able to differentiate upon LIF withdrawal (Fig. 4A and E). These data contrast with the function of other KDMs expressed in ES cells. KDM3A and KDM4C, whose expression is driven by Oct-4, are required for continued ES cell pluripotency by preventing the accumulation of H3K9me3 at genes such as the Nanog gene (35). ES cell differentiation is a complex process which requires the simultaneous activation of lineage-specific genes and the repression of stem cell factors such as Oct-4 and Nanog. The Oct-4 promoter shows a dramatic decrease in H3K4me within the first 48 h of retinoic acid-mediated differentiation in embryonic carcinoma cells (12), which suggests a potential role for LSD1. However, stem cell markers including Oct-4, Nanog, and Rex1 are all repressed in embryoid bodies derived from $LSD1^{\Delta 3/\Delta 3}$ cells (Fig. 4E), implying that either another KDM is responsible for the demethylation of H3K4me/me2 at these genes or loss of this positive mark is not essential for repression.

LSD1 regulates the transcriptome during embryonic development. Comparative microarray analysis of $Lsd1^{Lox/\Delta 3}$ versus $Lsd1^{\Delta 3/\Delta 3}$ ES cells revealed that 60% more genes were upregulated (362) than downregulated (226), suggesting loss of a repressive factor (Fig. 5A; see Table S1 in the supplemental material). This is consistent with a reduction in levels of the corepressor, CoREST, and a global increase in H3K9 and H3K56 acetylation (Fig. 3B and E). These changes occur independently of the reduced genomic methylation levels observed in late-passage ES cells lacking LSD1 (Fig. 2H) (54). Interestingly, we observed an enrichment of bivalent genes among those upregulated by loss of LSD1 (Fig. 5E), implying a role for LSD1 in the balance of H3K4me3 and H3K27me3 modifications. ChIP-on-chip and ChIP-Seq data sets from Orford et al. (40) and Meissner et al. (37) indicate that the vast majority of promoters positive for H3K4me3, are also positive for H3K4me2 in ES cells. While multipotent hematopoietic and neuronal precursor cells have a subset of "poised" $H3K4me2^{+}/H3K4me3^{-}$ genes, these seem to be absent from ES cells. The data in Fig. 5E therefore represents both genes with H3K4me3 and H3K4me2 (the LSD1 substrate). The number of 588 affected transcripts is relatively small in comparison to the number of potential LSD1 gene targets identified in three different large-scale ChIP studies in murine erythroleukemia (MEL) cells (5,191 targets) (43) and MCF7 cells (4,212 targets [18] and 1,913 targets [56]). While this is a comparison of two different systems (stem cells and somatic cells), it suggests that LSD1 activity may not be essential for the repression (or potentially activation) of all of these targets. It is also noteworthy that Gfi1/Gfi1b and the estrogen receptor, factors which determine LSD1 recruitment to target promoters, in these studies are not expressed in ES cells. Among the altered transcripts, we identified a number of transcription factors with roles in anterior/posterior pattern formation and tissue-specific development, including brachyury, Hoxb7, Hoxd8, RARγ, and Gli2 (Fig. 5B and C; see Table S1 in the supplemental material), implying that LSD1 is required to regulate multiple differentiation programs in pluripotent cells. However, altered expression of these factors and a significant enrichment for genes with a muscle-specific function (Fig. 5D) do not cause loss of pluripotency in $Lsd1^{\Delta 3/\Delta 3}$ cells (as discussed above). In this regard, the identification of brachyury as a direct target of LSD1 is informative. Loss of LSD1 causes a 3- to 5-fold increase of brachyury mRNA, whereas the induction of differentiation results in a 22-fold increase in transcriptional levels (Fig. 6A). Therefore, removal of a repressive factor (LSD1) results in a modest increase in gene expression, which is amplified by transcriptional activation during differentiation. It should be stressed that *brachyury*, although important for embryonic development, is only one of 588 aberrantly expressed genes and that a combination of conflicting developmental cues are likely to cause embryonic lethality in embryos with LSD1 deleted (54, 55) (Fig. 1C).

To determine the molecular mechanism underlying the essential requirement for LSD1 in the developing mouse embryo, we have shown that LSD1 is expressed exclusively in the epiblast following implantation. Analysis of ES cells reveals that LSD1 regulates the transcriptome, in part through the stabilization of CoREST protein, as an integral component of the LSD1/CoREST/HDAC complex. Loss of LSD1 demethylase activity results in the premature activation of brachyury, a key regulator of mesoderm formation, and a number of other transcription factors with roles in anterior/posterior pattern formation. Thus, LSD1 is required to coordinate gene expression as a key catalytic and structural component of the LSD1/CoREST/HDAC complex in early embryonic development.

ACKNOWLEDGMENTS

We extend our thanks to John Schwabe, Felix Beck, and Salvador Macip for useful discussions and critical reading of the manuscript. We thank Sally Edwards and Frances Law for technical assistance with ES cell culture and isolation of *Lsd1* gene trap embryos. E14 ES cells and the *ROSA26-CreER* targeting vector were kindly provided by David Adams.

This work was supported by a Medical Research Council (MRC) studentship to C.T.F. and a Career Development Award (G0600135) to S.M.C.

REFERENCES

1. **Azuara, V., P. Perry, S. Sauer, M. Spivakov, H. F. Jorgensen, R. M. John, M. Gouti, M. Casanova, G. Warnes, M. Merkenschlager, and A. G. Fisher.** 2006. Chromatin signatures of pluripotent cell lines. Nat. Cell Biol. **8:**532–538.
2. **Ballas, N., E. Battaglioli, F. Atouf, M. E. Andres, J. Chenoweth, M. E. Anderson, C. Burger, M. Moniwa, J. R. Davie, W. J. Bowers, H. J. Federoff, D. W. Rose, M. G. Rosenfeld, P. Brehm, and G. Mandel.** 2001. Regulation of neuronal traits by a novel transcriptional complex. Neuron **31:**353–365.
3. **Bannister, A. J., P. Zegerman, J. F. Partridge, E. A. Miska, J. O. Thomas, R. C. Allshire, and T. Kouzarides.** 2001. Selective recognition of methylated lysine 9 on histone H3 by the HP1 chromo domain. Nature **410:**120–124.
4. **Barlev, N. A., L. Liu, N. H. Chehab, K. Mansfield, K. G. Harris, T. D. Halazonetis, and S. L. Berger.** 2001. Acetylation of p53 activates transcription through recruitment of coactivators/histone acetyltransferases. Mol. Cell **8:**1243–1254.
5. **Bernstein, B. E., T. S. Mikkelsen, X. Xie, M. Kamal, D. J. Huebert, J. Cuff,**

B. Fry, A. Meissner, M. Wernig, K. Plath, R. Jaenisch, A. Wagschal, R. Feil, S. L. Schreiber, and E. S. Lander. 2006. A bivalent chromatin structure marks key developmental genes in embryonic stem cells. Cell **125:**315–326.
6. **Chen, Y., Y. Yang, F. Wang, K. Wan, K. Yamane, Y. Zhang, and M. Lei.** 2006. Crystal structure of human histone lysine-specific demethylase 1 (LSD1). Proc. Natl. Acad. Sci. U. S. A. **103:**13956–13961.
7. **Christensen, J., K. Agger, P. A. Cloos, D. Pasini, S. Rose, L. Sennels, J. Rappsilber, K. H. Hansen, A. E. Salcini, and K. Helin.** 2007. RBP2 belongs to a family of demethylases, specific for tri-and dimethylated lysine 4 on histone 3. Cell **128:**1063–1076.
8. **Ciccone, D. N., H. Su, S. Hevi, F. Gay, H. Lei, J. Bajko, G. Xu, E. Li, and T. Chen.** 2009. KDM1B is a histone H3K4 demethylase required to establish maternal genomic imprints. Nature **461:**415–418.
9. **Cloos, P. A., J. Christensen, K. Agger, and K. Helin.** 2008. Erasing the methyl mark: histone demethylases at the center of cellular differentiation and disease. Genes Dev. **22:**1115–1140.
10. **Das, C., M. S. Lucia, K. C. Hansen, and J. K. Tyler.** 2009. CBP/p300-mediated acetylation of histone H3 on lysine 56. Nature **459:**113–117.
11. **Dovey, O. M., C. T. Foster, and S. M. Cowley.** 2010. Histone deacetylase 1 (HDAC1), but not HDAC2, controls embryonic stem cell differentiation. Proc. Natl. Acad. Sci. U. S. A. **107:**8242–8247.
12. **Feldman, N., A. Gerson, J. Fang, E. Li, Y. Zhang, Y. Shinkai, H. Cedar, and Y. Bergman.** 2006. G9a-mediated irreversible epigenetic inactivation of Oct-3/4 during early embryogenesis. Nat. Cell Biol. **8:**188–194.
13. **Forneris, F., C. Binda, A. Adamo, E. Battaglioli, and A. Mattevi.** 2007. Structural basis of LSD1-CoREST selectivity in histone H3 recognition. J. Biol. Chem. **282:**20070–20074.
14. **Forneris, F., C. Binda, E. Battaglioli, and A. Mattevi.** 2008. LSD1: oxidative chemistry for multifaceted functions in chromatin regulation. Trends Biochem. Sci. **33:**181–189.
15. **Forneris, F., C. Binda, A. Dall'Aglio, M. W. Fraaije, E. Battaglioli, and A. Mattevi.** 2006. A highly specific mechanism of histone H3-K4 recognition by histone demethylase LSD1. J. Biol. Chem. **281:**35289–35295.
16. **Forneris, F., C. Binda, M. A. Vanoni, E. Battaglioli, and A. Mattevi.** 2005. Human histone demethylase LSD1 reads the histone code. J. Biol. Chem. **280:**41360–41365.
17. **Forneris, F., C. Binda, M. A. Vanoni, A. Mattevi, and E. Battaglioli.** 2005. Histone demethylation catalysed by LSD1 is a flavin-dependent oxidative process. FEBS Lett. **579:**2203–2207.
18. **Garcia-Bassets, I., Y. S. Kwon, F. Telese, G. G. Prefontaine, K. R. Hutt, C. S. Cheng, B. G. Ju, K. A. Ohgi, J. Wang, L. Escoubet-Lozach, D. W. Rose, C. K. Glass, X. D. Fu, and M. G. Rosenfeld.** 2007. Histone methylation-dependent mechanisms impose ligand dependency for gene activation by nuclear receptors. Cell **128:**505–518.
19. **Hakimi, M. A., D. A. Bochar, J. Chenoweth, W. S. Lane, G. Mandel, and R. Shiekhattar.** 2002. A core-BRAF35 complex containing histone deacetylase mediates repression of neuronal-specific genes. Proc. Natl. Acad. Sci. U. S. A. **99:**7420–7425.
20. **Huang, D. W., B. T. Sherman, and R. A. Lempicki.** 2009. Systematic and integrative analysis of large gene lists using DAVID bioinformatics resources. Nat. Protoc. **4:**44–57.
21. **Huang, J., R. Sengupta, A. B. Espejo, M. G. Lee, J. A. Dorsey, M. Richter, S. Opravil, R. Shiekhattar, M. T. Bedford, T. Jenuwein, and S. L. Berger.** 2007. p53 is regulated by the lysine demethylase LSD1. Nature **449:**105–108.
22. **Humphrey, G. W., Y. Wang, V. R. Russanova, T. Hirai, J. Qin, Y. Nakatani, and B. H. Howard.** 2001. Stable histone deacetylase complexes distinguished by the presence of SANT domain proteins CoREST/kiaa0071 and Mta-L1. J. Biol. Chem. **276:**6817–6824.
23. **Iwase, S., F. Lan, P. Bayliss, L. de la Torre-Ubieta, M. Huarte, H. H. Qi, J. R. Whetstine, A. Bonni, T. M. Roberts, and Y. Shi.** 2007. The X-linked mental retardation gene SMCX/JARID1C defines a family of histone H3 lysine 4 demethylases. Cell **128:**1077–1088.
24. **Jenuwein, T., and C. D. Allis.** 2001. Translating the histone code. Science **293:**1074–1080.
25. **Karytinos, A., F. Forneris, A. Profumo, G. Ciossani, E. Battaglioli, C. Binda, and A. Mattevi.** 2009. A novel mammalian flavin-dependent histone demethylase. J. Biol. Chem. **284:**17775–17782.
26. **Klose, R. J., Q. Yan, Z. Tothova, K. Yamane, H. Erdjument-Bromage, P. Tempst, D. G. Gilliland, Y. Zhang, and W. G. Kaelin, Jr.** 2007. The retinoblastoma binding protein RBP2 is an H3K4 demethylase. Cell **128:**889–900.
27. **Kouzarides, T.** 2007. Chromatin modifications and their function. Cell **128:**693–705.
28. **Ku, M., R. P. Koche, E. Rheinbay, E. M. Mendenhall, M. Endoh, T. S. Mikkelsen, A. Presser, C. Nusbaum, X. Xie, A. S. Chi, M. Adli, S. Kasif, L. M. Ptaszek, C. A. Cowan, E. S. Lander, H. Koseki, and B. E. Bernstein.** 2008. Genomewide analysis of PRC1 and PRC2 occupancy identifies two classes of bivalent domains. PLoS Genet. **4:**e1000242.
29. **Lachner, M., D. O'Carroll, S. Rea, K. Mechtler, and T. Jenuwein.** 2001. Methylation of histone H3 lysine 9 creates a binding site for HP1 proteins. Nature **410:**116–120.
30. **Lan, F., R. E. Collins, R. De Cegli, R. Alpatov, J. R. Horton, X. Shi, O. Gozani, X. Cheng, and Y. Shi.** 2007. Recognition of unmethylated histone H3 lysine 4 links BHC80 to LSD1-mediated gene repression. Nature **448:**718–722.
31. **Lee, M. G., J. Norman, A. Shilatifard, and R. Shiekhattar.** 2007. Physical and functional association of a trimethyl H3K4 demethylase and Ring6a/MBLR, a polycomb-like protein. Cell **128:**877–887.
32. **Lee, M. G., C. Wynder, D. A. Bochar, M. A. Hakimi, N. Cooch, and R. Shiekhattar.** 2006. Functional interplay between histone demethylase and deacetylase enzymes. Mol. Cell. Biol. **26:**6395–6402.
33. **Lee, M. G., C. Wynder, N. Cooch, and R. Shiekhattar.** 2005. An essential role for CoREST in nucleosomal histone 3 lysine 4 demethylation. Nature **437:**432–435.
34. **Liang, G., R. J. Klose, K. E. Gardner, and Y. Zhang.** 2007. Yeast Jhd2p is a histone H3 Lys4 trimethyl demethylase. Nat. Struct. Mol. Biol. **14:**243–245.
35. **Loh, Y. H., W. Zhang, X. Chen, J. George, and H. H. Ng.** 2007. Jmjd1a and Jmjd2c histone H3 Lys 9 demethylases regulate self-renewal in embryonic stem cells. Genes Dev. **21:**2545–2557.
36. **McGraw, S., C. Vigneault, and M. A. Sirard.** 2007. Temporal expression of factors involved in chromatin remodeling and in gene regulation during early bovine in vitro embryo development. Reproduction **133:**597–608.
37. **Meissner, A., T. S. Mikkelsen, H. Gu, M. Wernig, J. Hanna, A. Sivachenko, X. Zhang, B. E. Bernstein, C. Nusbaum, D. B. Jaffe, A. Gnirke, R. Jaenisch, and E. S. Lander.** 2008. Genome-scale DNA methylation maps of pluripotent and differentiated cells. Nature **454:**766–770.
38. **Metzger, E., M. Wissmann, N. Yin, J. M. Muller, R. Schneider, A. H. Peters, T. Gunther, R. Buettner, and R. Schule.** 2005. LSD1 demethylates repressive histone marks to promote androgen-receptor-dependent transcription. Nature **437:**436–439.
39. **Mikkelsen, T. S., M. Ku, D. B. Jaffe, B. Issac, E. Lieberman, G. Giannoukos, P. Alvarez, W. Brockman, T. K. Kim, R. P. Koche, W. Lee, E. Mendenhall, A. O'Donovan, A. Presser, C. Russ, X. Xie, A. Meissner, M. Wernig, R. Jaenisch, C. Nusbaum, E. S. Lander, and B. E. Bernstein.** 2007. Genome-wide maps of chromatin state in pluripotent and lineage-committed cells. Nature **448:**553–560.
40. **Orford, K., P. Kharchenko, W. Lai, M. C. Dao, D. J. Worhunsky, A. Ferro, V. Janzen, P. J. Park, and D. T. Scadden.** 2008. Differential H3K4 methylation identifies developmentally poised hematopoietic genes. Dev. Cell **14:**798–809.
41. **Rudolph, T., M. Yonezawa, S. Lein, K. Heidrich, S. Kubicek, C. Schafer, S. Phalke, M. Walther, A. Schmidt, T. Jenuwein, and G. Reuter.** 2007. Heterochromatin formation in Drosophila is initiated through active removal of H3K4 methylation by the LSD1 homolog SU(VAR)3–3. Mol. Cell **26:**103–115.
42. **Ruthenburg, A. J., H. Li, D. J. Patel, and C. D. Allis.** 2007. Multivalent engagement of chromatin modifications by linked binding modules. Nat. Rev. Mol. Cell Biol. **8:**983–994.
43. **Saleque, S., J. Kim, H. M. Rooke, and S. H. Orkin.** 2007. Epigenetic regulation of hematopoietic differentiation by Gfi-1 and Gfi-1b is mediated by the cofactors CoREST and LSD1. Mol. Cell **27:**562–572.
44. **Shechter, D., H. L. Dormann, C. D. Allis, and S. B. Hake.** 2007. Extraction, purification and analysis of histones. Nat. Protoc. **2:**1445–1457.
45. **Shi, Y., F. Lan, C. Matson, P. Mulligan, J. R. Whetstine, P. A. Cole, R. A. Casero, and Y. Shi.** 2004. Histone demethylation mediated by the nuclear amine oxidase homolog LSD1. Cell **119:**941–953.
46. **Shi, Y., J. Sawada, G. Sui, B. el Affar, J. R. Whetstine, F. Lan, H. Ogawa, M. P. Luke, and Y. Nakatani.** 2003. Coordinated histone modifications mediated by a CtBP co-repressor complex. Nature **422:**735–738.
47. **Shi, Y., and J. R. Whetstine.** 2007. Dynamic regulation of histone lysine methylation by demethylases. Mol. Cell **25:**1–14.
48. **Shi, Y. J., C. Matson, F. Lan, S. Iwase, T. Baba, and Y. Shi.** 2005. Regulation of LSD1 histone demethylase activity by its associated factors. Mol. Cell **19:**857–864.
49. **Skarnes, W. C., H. von Melchner, W. Wurst, G. Hicks, A. S. Nord, T. Cox, S. G. Young, P. Ruiz, P. Soriano, M. Tessier-Lavigne, B. R. Conklin, W. L. Stanford, and J. Rossant.** 2004. A public gene trap resource for mouse functional genomics. Nat. Genet. **36:**543–544.
50. **Smith, A. G.** 2001. Embryo-derived stem cells: of mice and men. Annu. Rev. Cell Dev. Biol. **17:**435–462.
51. **Snow, M. H. L.** 1977. Gastrulation in the mouse: growth and regionalization of the epiblast. J. Embryol. Exp. Morphol. **42:**293–303.
52. **Su, A. I., T. Wiltshire, S. Batalov, H. Lapp, K. A. Ching, D. Block, J. Zhang, R. Soden, M. Hayakawa, G. Kreiman, M. P. Cooke, J. R. Walker, and J. B. Hogenesch.** 2004. A gene atlas of the mouse and human protein-encoding transcriptomes. Proc. Natl. Acad. Sci. U. S. A. **101:**6062–6067.
53. **Tjeertes, J. V., K. M. Miller, and S. P. Jackson.** 2009. Screen for DNA-damage-responsive histone modifications identifies H3K9Ac and H3K56Ac in human cells. EMBO J. **28:**1878–1889.
54. **Wang, J., S. Hevi, J. K. Kurash, H. Lei, F. Gay, J. Bajko, H. Su, W. Sun, H. Chang, G. Xu, F. Gaudet, E. Li, and T. Chen.** 2009. The lysine demethylase LSD1 (KDM1) is required for maintenance of global DNA methylation. Nat. Genet. **41:**125–129.
55. **Wang, J., K. Scully, X. Zhu, L. Cai, J. Zhang, G. G. Prefontaine, A. Krones, K. A. Ohgi, P. Zhu, I. Garcia-Bassets, F. Liu, H. Taylor, J. Lozach, F. L.**

Jayes, K. S. Korach, C. K. Glass, X. D. Fu, and M. G. Rosenfeld. 2007. Opposing LSD1 complexes function in developmental gene activation and repression programmes. Nature **446:**882–887.

56. **Wang, Y., H. Zhang, Y. Chen, Y. Sun, F. Yang, W. Yu, J. Liang, L. Sun, X. Yang, L. Shi, R. Li, Y. Li, Y. Zhang, Q. Li, X. Yi, and Y. Shang.** 2009. LSD1 is a subunit of the NuRD complex and targets the metastasis programs in breast cancer. Cell **138:**660–672.
57. **Wissmann, M., N. Yin, J. M. Muller, H. Greschik, B. D. Fodor, T. Jenuwein, C. Vogler, R. Schneider, T. Gunther, R. Buettner, E. Metzger, and R. Schule.** 2007. Cooperative demethylation by JMJD2C and LSD1 promotes androgen receptor-dependent gene expression. Nat. Cell Biol. **9:**347–353.
58. **Wu, C., C. Orozco, J. Boyer, M. Leglise, J. Goodale, S. Batalov, C. L. Hodge, J. Haase, J. Janes, J. W. Huss III, and A. I. Su.** 2009. BioGPS: an extensible and customizable portal for querying and organizing gene annotation resources. Genome Biol. **10:**R130.
59. **Xie, W., C. Song, N. L. Young, A. S. Sperling, F. Xu, R. Sridharan, A. E. Conway, B. A. Garcia, K. Plath, A. T. Clark, and M. Grunstein.** 2009. Histone H3 lysine 56 acetylation is linked to the core transcriptional network in human embryonic stem cells. Mol. Cell **33:**417–427.
60. **Yang, M., C. B. Gocke, X. Luo, D. Borek, D. R. Tomchick, M. Machius, Z. Otwinowski, and H. Yu.** 2006. Structural basis for CoREST-dependent demethylation of nucleosomes by the human LSD1 histone demethylase. Mol. Cell **23:**377–387.
61. **Yang, X. J., and E. Seto.** 2008. The Rpd3/Hda1 family of lysine deacetylases: from bacteria and yeast to mice and men. Nat. Rev. Mol. Cell Biol. **9:**206–218.
62. **You, A., J. K. Tong, C. M. Grozinger, and S. L. Schreiber.** 2001. CoREST is an integral component of the CoREST-human histone deacetylase complex. Proc. Natl. Acad. Sci. U. S. A. **98:**1454–1458.
63. **Zeng, P. Y., C. R. Vakoc, Z. C. Chen, G. A. Blobel, and S. L. Berger.** 2006. In vivo dual cross-linking for identification of indirect DNA-associated proteins by chromatin immunoprecipitation. Biotechniques **41:**694, 696, 698.